American Mineralogist, Volume 62, pages 812–817, 1977

The crystal structure of phosphophyllite

RODERICK J. HILL

Department of Geological Sciences
Virginia Polytechnic Institute and State University
Blacksburg, Virginia 24061

Abstract

Phosphophyllite from Potosi, Bolivia, $Zn_2Fe(PO_4)_2 \cdot 4H_2O$, is monoclinic and crystallizes in space group $P2_1/c$, with a = 10.378(3), b = 5.084(1), c = 10.553(3) A, β = 121.14(2)°, and Z = 2. The structure has been solved by Patterson and Fourier methods from 1999 Zr-filtered Mo$K\alpha$ data and refined by full matrix least-squares (including the hydrogen atoms) to R = 0.032 (R_w = 0.035). The framework consists of $[Zn_2P_2O_7]$ tetrahedral sheets identical to those in hopeite, interleaved with $[FeO \cdot 4H_2O]$ octahedral sheets similar to those in parahopeite.

Introduction

Phosphophyllite from Hagendorf, Bavaria, $Zn_2(Fe,Mn)(PO_4)_2 \cdot 4H_2O$, was first described by Laubmann and Steinmetz (1920), but has been documented at relatively few other localities since then (Hill, 1976). Nevertheless, a large number of studies have suggested close relationships between the crystal structure of phosphophyllite and that of hopeite (Steinmetz, 1926; Wolfe, 1940; Gamidov *et al.*, 1963; Liebau, 1965; Kawahara *et al.*, 1973), and parahopeite (Kumbasar and Finney, 1968; Chao, 1969). Although the topology of hopeite and parahopeite is now known with some degree of precision (Hill and Jones, 1976; Chao, 1969), the phosphophyllite structure has been determined from two-dimensional X-ray data only (Kleber *et al.*, 1961), with the y coordinates estimated on the basis of interatomic distances within the inferred coordination polyhedra. Moreover, the framework determined by Kleber *et al.* contains a number of unusually short O···O nonbonded distances, and one distance which arises from the sharing of an edge between a ZnO_4 and a PO_4 tetrahedron. Based on an alternative interpretation of the published [010] projection, Hill (1975) proposed a new framework with more reasonable O···O distances and no shared edges. The new model was refined by the method of distance least-squares (Meier and Villiger, 1969) and converged to a structure essentially identical, except in the vicinity of the octahedral sites, to that of hopeite. The present three-dimensional X-ray refinement was initiated in order to determine which of the above models pertains to phosphophyllite.

Experimental

A roughly equidimensional cleavage fragment of phosphophyllite from Potosi, Bolivia (crystal volume = 5.6 × 10^{-6} cm^3) was oriented with the c axis parallel to the ϕ axis of a Picker FACS 1 four-circle diffractometer. Detailed chemical, optical, and X-ray data for material from this locality have been reported by Hill (1976); unit-cell dimensions from that study have been included in the abstract.[1] X-ray intensity data for the structure analysis were collected at 24°C using Zr-filtered Mo$K\alpha$ radiation (λ = 0.71069 A) and a 2θ scan rate of 2° per minute. Backgrounds were determined from 10-second stationary counts at both ends of each dispersion-corrected (Alexander and Smith, 1964) scan range (minimum width = 2.4° in 2θ). A total of 6285 reflections with $2\theta \lesssim 75°$ and $l \geq 0$ were measured, using three reflections to monitor instrument and crystal stability at frequent intervals; these showed no significant change. Systematic extinctions appropriate to space group $P2_1/c$ were removed, and the resultant data corrected for background, Lorentz, polarization, and absorption (based on actual crystal shape and a μ value of 70.22 cm^{-1}) effects. Symmetry-equivalent and multiply-measured reflections were averaged (by weight) to yield 2482 unique structure factors, each

[1] *esd*'s, given in parentheses, refer to the last decimal place.

with a standard deviation estimated from the equation $\sigma = [\sigma_I^2 + (0.03I)^2]^{0.5}/2I^{0.5}$, where I is the corrected raw intensity and σ_I is derived from counting and averaging statistics. Of these data only those 1999 observations with $I > 2\sigma_I$ were included in the subsequent least-squares refinement.

Structure determination and refinement

The Fe and Zn atoms were located from the Patterson function, and the P and O atoms from partially phased Fourier syntheses. These atoms were refined by least-squares minimization of $\Sigma w(|F_0| - |F_c|)^2$, where F_0 and F_c are the observed and calculated structure factors, and $w = 1/\sigma^2$. Refinement with isotropic temperature factors converged with a conventional R value of 0.055. Refinement with anisotropic temperature factors[2] and the inclusion of an isotropic extinction parameter (g), as defined and scaled by Coppens and Hamilton (1970), further reduced R to 0.033.

A Fourier difference synthesis utilizing only those data with $\sin\theta/\lambda < 0.4$ A^{-1} was computed, and peaks ranging from 0.49 to 0.88eA^{-3} were found for the four hydrogen atoms in the asymmetric unit. There were also a small number of other peaks with maximum density 1.35eA^{-3} (less than 10% of the magnitude of an O atom peak), but these were all located well within the coordination spheres of Zn, Fe, and P, and were interpreted as regions of charge deformation due to chemical bonding. Full matrix refinement, including the H atom positional and isotropic thermal parameters and using all 1999 reflections, then proceeded smoothly to convergence (recommended shifts in the final cycle were less than one tenth of the appropriate *esd*). The final values of R and R_w[3] were 0.032 and 0.035 respectively (0.048 and 0.038 for the entire data set of 2482 structure factors), with the error in an observation of unit weight = 1.29. Only 33 reflections were affected more than 3 percent by $g = 2.2(2)$. Values for F_0 and F_c ($\times$ 10) are listed in Table 1.[4] Atomic coordinates and thermal parameters along with their standard deviations estimated from the inverted full matrix are given in Table 2. The r.m.s. components of thermal displacement, and thermal ellipsoid orientations appear in Table 3.

[2] The form of the anisotropic thermal ellipsoid is $\exp[-(\beta_{11}h^2 + \beta_{22}k^2 + \beta_{33}l^2 + 2\beta_{12}hk + 2\beta_{13}hl + 2\beta_{23}kl)]$.

[3] $R_w = [\Sigma w(|F_0| - |F_c|)^2/\Sigma wF_0^2]^{1/2}$

[4] To obtain a copy of Table 1, order Document AM-77-046 from the Mineralogical Society of America, Business Office, 1909 K St. N.W., Washington, D.C. 20006. Please remit in advance $1.00 for a copy of the microfiche.

Scattering factors for Zn, Fe, P, and O (neutral atoms) were obtained from *International Tables for X-ray Crystallography* (1974) and were corrected for both real and imaginary anomalous dispersion components. For H, the spherical scattering factor suggested by Stewart *et al.* (1965) was used. Programs utilized for solution, refinement and geometry calculations were local modifications of DATALIB, DATASORT, FOURIER, ORXFLS3, ORFFE3, and ORTEP2.[5]

Discussion of the structure

Phosphophyllite crystallizes with the topology displayed in Figure 1 and the bonding dimensions summarized in Table 4. These results confirm the three-dimensional framework proposed by Hill (1975) using the method of distance least-squares (mean values of Δx, Δy, and Δz for the two refinements are 0.06, 0.05, and 0.15 A respectively), although the two-dimensional structure reported by Kleber *et al.* (1961) remains essentially intact (mean values for Δx and Δz are 0.05 and 0.11 A).

In detail, the structure consists of puckered sheets of corner-sharing tetrahedra of O atoms parallel to (100), interleaved with sheets of face-sharing vacant and occupied O octahedra. Zn and P are distributed equally among the tetrahedral sites to produce a network of three- and four-membered rings identical to that in hopeite (Hill and Jones, 1976). Not unexpectedly, therefore, the deviations from ideal tetrahedron shape within the layers are very similar in both minerals. The longer bonds from Zn and P to the trigonally coordinated O(6) atom, relative to other bonds within each tetrahedron, correlate with the larger sum of electrostatic bond strengths (Baur, 1970) and with the narrower valence angles (Louisnathan and Gibbs, 1972) associated with O(6) as a result of ring formation.

The Fe atom occupies one-quarter of the available sites in the octahedral sheet (the remaining sites are vacant), giving rise to a fairly regular polyhedron with mean bond lengths close to the value 2.17 A expected for Fe^{2+} in octahedral coordination (Shannon and Prewitt, 1969). The O(3) atom of the PO_4 group serves as the major link between the tetrahedral and octahedral sheets. In phosphophyllite this atom has a *trans* relationship with respect to the other (water) O atoms of the octahedron, consistent with the centrosymmetry of the Fe site. In hopeite, however, the (Zn) octahedron has mirror symme-

[5] All programs are included in the *World List of Crystallographic Computer Programs* (3rd ed. and supplements).

Table 2. Fractional atomic coordinates and temperature factor coefficients for phosphophyllite

Atom	x	y	z	β_{11} or B	β_{22}	β_{33}	β_{12}	β_{13}	β_{23}
Fe	0	0	0	286(5)	689(14)	250(5)	51(7)	139(4)	47(7)
Zn	50024(3)	31002(5)	35646(3)	321(3)	559(8)	249(3)	-31(4)	174(2)	-4(4)
P	68924(6)	28707(11)	19476(6)	183(5)	478(17)	218(5)	7(8)	111(5)	-28(8)
O(1)	-46(3)	2958(4)	1392(3)	75(3)	130(7)	59(2)	-35(4)	49(2)	-35(3)
O(2)	1803(3)	2897(5)	5030(3)	51(2)	145(7)	78(3)	-3(4)	45(2)	-8(4)
O(3)	8542(2)	2582(4)	3158(2)	22(2)	85(5)	33(2)	4(3)	5(2)	-11(2)
O(4)	3526(2)	728(3)	3420(2)	41(2)	67(5)	62(2)	-17(3)	32(2)	-16(3)
O(5)	6617(2)	1323(4)	582(2)	35(2)	112(6)	21(2)	17(3)	12(1)	-7(3)
O(6)	5860(2)	1527(3)	2445(2)	44(2)	79(5)	43(2)	-19(3)	34(2)	-17(3)
H(13)	-30(4)	276(8)	195(4)	2.0(8)					
H(13^i)	54(6)	403(11)	177(6)	4.4(12)					
H(25)	231(8)	358(17)	491(8)	8(2)					
H(2)	219(8)	154(17)	547(9)	10(2)					

* *Positional and thermal parameters × 10^5 for Fe, Zn, P; × 10^4 for O. H atom positional parameters × 10^3. Parenthesized figures represent the e.s.d. in terms of the least significant figure to the left.*

Table 3. Magnitudes and orientations of the principal axes of thermal ellipsoids in phosphophyllite

Atom	Axis	R.m.s. displacement (Å)*	Angle in degrees to +a	+b	+c
Fe	1	0.091(1)	99(3)	28(3)	108(4)
	2	0.103(1)	57(6)	108(4)	162(4)
	3	0.109(1)	35(6)	69(3)	93(6)
Zn	1	0.085(1)	76(2)	16(3)	104(3)
	2	0.094(1)	55(1)	104(3)	165(3)
	3	0.114(1)	38(1)	97(1)	84(1)
P	1	0.076(1)	63(7)	151(7)	112(4)
	2	0.085(1)	151(7)	115(7)	75(5)
	3	0.096(1)	98(4)	104(3)	27(4)
O(1)	1	0.107(4)	102(8)	41(7)	50(9)
	2	0.125(4)	144(4)	119(8)	46(9)
	3	0.190(3)	57(2)	116(2)	71(2)
O(2)	1	0.114(4)	9(6)	96(7)	128(2)
	2	0.137(4)	97(7)	170(5)	93(5)
	3	0.181(3)	84(2)	98(3)	38(2)
O(3)	1	0.088(4)	48(6)	87(14)	74(5)
	2	0.100(3)	74(11)	160(4)	108(5)
	3	0.145(3)	133(3)	109(3)	25(3)
O(4)	1	0.085(4)	71(5)	22(4)	90(3)
	2	0.120(3)	161(5)	72(5)	57(3)
	3	0.162(3)	90(3)	102(2)	33(3)
O(5)	1	0.087(4)	112(7)	63(6)	27(5)
	2	0.102(4)	126(5)	56(6)	101(9)
	3	0.143(3)	44(3)	46(3)	115(3)
O(6)	1	0.088(4)	29(10)	70(30)	139(23)
	2	0.093(4)	82(29)	151(22)	118(28)
	3	0.151(3)	63(2)	111(2)	63(2)
H(13)	-	0.16(3)			
H(13^i)	-	0.24(3)			
H(25)	-	0.32(4)			
H(2)	-	0.35(4)			

* *Parenthesized figures represent the e.s.d. in terms of the least significant figure to the left.*

try and the corresponding bridging O atom occupies a *cis* position, thereby giving rise to a primitive/orthohexagonal relationship between the unit cells of the two minerals (Wolfe, 1940; Gamidov *et al.*, 1963). Since the tetrahedral portions of both frameworks are identical, this relationship allows the structure of hopeite to be obtained in its entirety by polysynthetic twinning of the phosphophyllite unit cell about the (100) plane (Gamidov *et al.*, 1963; Kawahara *et al.*, 1973). In fact, the mode of coordination of the Fe atom in phosphophyllite is the same as that of the octahedrally-coordinated Zn atom in the closely related mineral parahopeite (Kumbasar and Finney, 1968; Chao, 1969), although the tetrahedral sheet is composed only of four-membered rings and the bridging atom is trigonally coordinated in the latter species. Indeed, the ability of the parahopeite structure to accommodate a significant amount of Fe (along with Mg and Mn) in the octahedral site (Hill and Milnes, 1974) lends support to the suggestion by Kawahara *et al.* (1973) that phosphophyllite, hopeite, and parahopeite may be considered to be trimorphous.

Anapaite, ludlamite, and switzerite are also members of Wolfe's (1940) family of the type $A_3(PO_4)_2 \cdot 4H_2O$. The first two species have crystal structures (Rumanova and Znamenskaya, 1960; Abrahams, 1966) unrelated to those of hopeite, parahopeite, and phosphophyllite, and although its structure is as yet undetermined, switzerite (Leavens and White, 1967) also appears to be unique within this

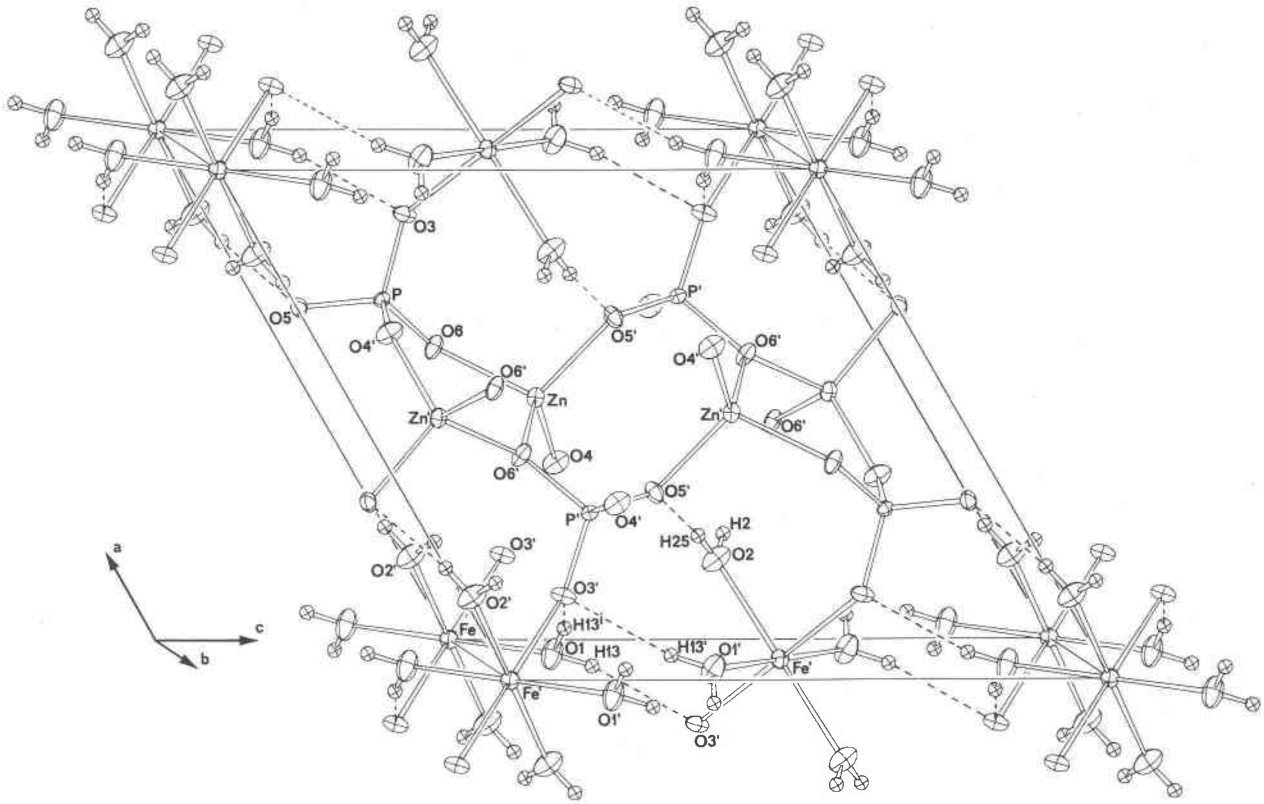

Fig 1. Unit-cell diagram of the phosphophyllite crystal structure. Thermal ellipsoids for all atoms (B for hydrogen set = 0.5 A^2) represent 50% probability surfaces. Hydrogen bonds are indicated by dashed lines. Atoms outside the asymmetric unit are labelled with superscript primes.

chemical group. However, a structural similarity between phosphophyllite and phosphosiderite (metastrengite), based on X-ray powder data, has been suggested by Strunz (1942) and subsequently confirmed by Moore (1966); the arrangement of PO_4 tetrahedra and Zn atoms is such that subcells within the phosphophyllite structure are closely related to portions of the phosphosiderite framework.

Hydrogen bonding

The distance and angle parameters describing the two water molecules and their associated hydrogen bonds are given in Table 4. All four O–H distances are within one *esd* of their average value, 0.76 A, and are about 0.20 A shorter than the corresponding average distance measured by neutron diffraction (Baur, 1972). Similar shifts of the apparent X-ray hydrogen position toward the atom to which it is bonded have been documented by a large number of workers (Stewart *et al.*, 1965; Hvoslef, 1968; Hanson *et al.*, 1973; Coppens, 1974), and are considered to reflect the relatively large distortion of the hydrogen atom electron density during formation of the O–H bond. Under these circumstances, little credence can be attached to the r.m.s. displacements (Table 3) derived from the hydrogen atom 'thermal' parameters, and for this reason no attempt has been made to apply a vibration correction to the O_d–H distances in Table 4.

Both hydrogen atoms in the O(1) water molecule participate in hydrogen bonds to O(3) across one of the vacant octahedra within the octahedral sheet. This configuration appears to be controlled by the nonlinearity of the Fe–O(3)–P linkage (132°) which brings O(3) closer to O(1) than any other oxygen atom. However, the O(1)–H$\cdots$O(3) angles also deviate from 180°, reflecting an attempt to reach a compromise with the bonding requirements of O(1). The resultant H–O(1)–H bond angle, 101(4)°, is close to the mean value of 109° documented for crystalline hydrates (Baur, 1972).

In contrast, the hydrogen atoms in the O(2) water molecule are directed toward the tetrahedral sheet. The H(25) atom participates in a single hydrogen

Table 4. Phosphophyllite interatomic distances and angles*

PO_4 tetrahedron		ZnO_4 tetrahedron		$FeO_2(H_2O)_4$ octahedron	
P-O(4)^{i}	1.508(2)	Zn-O(4)	1.894(2)	Fe-O(1)	2.119(2) × 2
O(3)	1.524(2)	O(5)^{ii}	1.933(2)	O(3)^{iii}	2.130(2) × 2
O(5)	1.534(2)	O(6)	1.979(2)	O(2)^{iv}	2.141(2) × 2
O(6)	1.572(2)	O(6)^{i}	1.996(2)	average =	2.130(2)
average =	1.534(1)	average =	1.950(1)	O(1)-O(3)^{iii}	3.060(3) × 2
O(4)^{i}-O(3)	2.498(3)	O(4)-O(5)^{ii}	3.190(3)	O(3)^{v}	2.949(3) × 2
O(5)	2.511(3)	O(6)	3.110(3)	O(2)^{iv}	3.060(3) × 2
O(6)	2.530(2)	O(6)^{i}	3.246(2)	O(2)^{vi}	2.964(3) × 2
O(3)-O(5)	2.485(3)	O(5)^{ii}-O(6)	3.175(3)	O(2)^{iv}-O(3)^{iii}	2.910(3) × 2
O(6)	2.537(3)	O(6)^{i}	3.227(3)	O(3)^{v}	3.127(3) × 2
O(5)-O(6)	2.468(3)	O(6)-O(6)^{i}	3.143(2)	average =	2.956(2)
average =	2.505(2)	average =	3.182(2)	∠O(1)-Fe-O(3)^{iii}	92.11(8) × 2
∠O(4)^{i}-P-O(3)	110.9(1)	∠O(4)-Zn-O(5)^{ii}	112.93(8)	O(3)^{v}	87.89(8) × 2
O(5)	111.3(1)	O(6)	106.85(7)	O(2)^{iv}	91.83(9) × 2
O(6)	110.4(1)	O(6)^{i}	113.09(8)	O(2)^{vi}	88.17(9) × 2
O(3)-P-O(5)	108.7(1)	O(5)^{ii}-Zn-O(6)	108.53(8)	O(2)^{iv}-Fe-O(3)^{iii}	85.89(8) × 2
O(6)	110.0(1)	O(6)^{i}	110.44(8)	O(3)^{v}	94.11(8) × 2
O(5)-P-O(6)	105.22(9)	O(6)-Zn-O(6)^{i}	104.48(5)	average =	90
average =	109.4(1)	average =	109.4(1)		

Water molecules

O_d	H	O_a	O_d-H	H···O_a	O_d···O_a	∠O_d-H···O_a	∠Fe-O_d-H	H···H	∠H-O_d-H
O(1)	H(13^{i})···	O(3)^{i}	0.75(6)	2.03(6)	2.724(3)	154(5)	125(4)	1.17(6)	101(4)
	H(13)···	O(3)^{vii}	0.77(4)	2.16(4)	2.913(3)	168(4)	125(4)		
O(2)	H(25)···	O(5)^{i}	0.70(8)	2.01(8)	2.690(3)	165(9)	119(8)	1.24(9)	110(7)
	H(2)		0.81(9)						

* *Distances and angles are quoted in Å and degrees respectively. Parenthesized figures represent the e.s.d. in terms of the last decimal place. Symmetry transformations for atoms outside the asymmetric unit:*

i. 1-x, 1/2+y, 1/2-z iii. 1-x, y-1/2, 1/2-z v. x-1, 1/2-y, z-1/2 vii. x-1, y, z
ii. x, 1/2-y, 1/2+z iv. -x, y-1/2, 1/2-z vi. x, 1/2-y, z-1/2

bond of normal dimensions to O(5), the nearest oxygen to O(2), but the hydrogen bonding scheme for H(2) is more difficult to determine: O(6), O(1) and O(3) are all more or less equidistant from H(2), while O(3), O(1) and O(4) give approximately equal values of O(2)···O_a. Moreover, all these distances are at the upper limit of the range of values observed for hydrogen bonds in other compounds (Baur, 1972). In addition, the balance of electrostatic bond strengths computed from the empirical curves of Brown and Shannon (1973), including the contributions of the hydrogen bonds from all atoms except H(2), indicates that O(3), O(4) and O(5) are underbonded by a small amount, while O(6) is slightly overbonded. I therefore conclude that the O(2) water molecule is anchored only by the H(25) hydrogen bond, thereby explaining the relatively higher standard errors and thermal parameters obtained for this group, especially H(2), during least-squares refinement. In spite of this, however, the H–O(2)–H angle is quite close to the expected value of 109°.

Although the symmetry of the $FeO_2(H_2O)_4$ octahedron in phosphophyllite is significantly different from that of the $ZnO_2(H_2O)_4$ octahedron in hopeite, the hydrogen bonding scheme proposed for the latter mineral by Whitaker (1975) is essentially analogous to the one determined in the present study. Small differences in atomic coordinates between the two structures have, however, stabilized a hydrogen bond between H(35) and O(5) in hopeite, whereas the equivalent atoms in phosphophyllite, H(2) and O(4), form no such association.

Acknowledgments

I am especially grateful to Dr. F. K. Ross of the Virginia Polytechnic Institute and State University Chemistry Department for his assistance during data collection and processing, and to the Research Division for defraying the computer costs. I acknowledge the support of a CSIRO postdoctoral studentship and grant DMR75-03879 from the Materials Research Division of the National Science Foundation.

References

Abrahams, S. C. (1966) Ferromagnetic and crystal structure of ludlamite, $Fe_3(PO_4)_2 \cdot 4H_2O$, at 4.2°K. *J. Chem. Phys.*, *44*, 2230–2237.

Alexander, L. E. and G. S. Smith (1964) Single-crystal diffractometry: the improvement of accuracy in intensity measurements. *Acta Crystallogr.*, *17*, 1195–1201.

Baur, W. H. (1970) Bond length variation and distorted coordination polyhedra in inorganic crystals. *Trans. Am. Crystallogr. Assoc.*, *6*, 129–155.

——— (1972) Prediction of hydrogen bonds and hydrogen atom positions in crystalline solids. *Acta Crystallogr.*, *B28*, 1456–1465.

Brown, I. D. and R. D. Shannon (1973) Empirical bond-strength–bond-length curves for oxides. *Acta Crystallogr.*, *A29*, 266–282.

Chao, G. Y. (1969) Refinement of the crystal structure of parahopeite. *Z. Kristallogr.*, *130*, 261–266.

Coppens, P. (1974) Some implications of combined X-ray and neutron diffraction studies. *Acta Crystallogr.*, *B30*, 255–261.

——— and W. C. Hamilton (1970) Anisotropic extinction corrections in the Zachariasen approximation. *Acta Crystallogr.*, *A26*, 71–83.

Gamidov, R. S., V. P. Golovachev, Kh.S. Mamedov and N. V. Belov (1963) Crystal structure of hopeite $Zn_3[PO_4]_2 \cdot 4H_2O$. *Dokl. Akad. Nauk SSSR*, *150*, 381–384 [transl. *Dokl. Acad. Sci. USSR*, *150*, 106–109 (1965)].

Hanson, J. C., L. C. Sieker and L. H. Jensen (1973) Sucrose: X-ray refinement and comparison with neutron refinement. *Acta Crystallogr.*, *B29*, 797–808.

Hill, R. J (1975) *The crystal structure of the mineral scholzite and a study of the crystal chemistry of zinc in some related phosphate and arsenate minerals.* Ph.D. Thesis, University of Adelaide, Adelaide, South Australia.

——— (1976) Crystal data for phosphophylite, $Zn_2Fe(PO_4)_2 \cdot 4H_2O$. *J. Appl. Crystallogr.*, *9*, 503–504.

——— and J. B. Jones (1976) The crystal structure of hopeite. *Am. Mineral.*, *61*, 987–995.

——— and A. R. Milnes (1974) Phosphate minerals from Reaphook Hill, Flinders Ranges, South Australia. *Mineral. Mag.*, *39*, 684–695.

Hvoslef, J. (1968) The crystal structure of L-ascorbic acid, 'Vitamin C.' I. The X-ray analysis. *Acta Crystallogr.*, *B24*, 23–35.

International Tables for X-ray Crystallography, Vol. IV (1974) Kynock, Birmingham, England, p. 99 and 149.

Kawahara, A., Y. Takano and M. Takahashi (1973) The structure of hopeite. *Mineral. J. (Japan)*, *7*, 289–297.

Kleber, W. F., F. Liebau and E. Piatkowiak (1961) Zur Struktur des Phosphophyllits, $Zn_2Fe[PO_4]_2 \cdot 4H_2O$. *Acta Crystallogr.*, *14*, 795.

Kumbasar, I., and J. J. Finney (1968) The crystal structure of parahopeite. *Mineral. Mag.*, *36*, 621–624.

Laubmann, H. and H. Steinmetz (1920) Der Pegmatit von Hagendorf. *Z. Kristallogr.*, *55*, 557–570.

Leavens, P. B. and J. S. White, Jr. (1967) Switzerite, $(Mn,Fe)_3(PO_4)_2 \cdot 4H_2O$, a new mineral. *Am. Mineral.*, *52*, 1595–1602.

Liebau, F. (1965) Zur Kristallstruktur des Hopeits, $Zn_3[PO_4]_2 \cdot 4H_2O$. *Acta Crystallogr.*, *18*, 352–354.

Louisnathan, S. J. and G. V. Gibbs (1972) Bond length variation in TO_4^{n-} tetrahedral oxyanions of the third row elements: T = Al, Si, P, S and Cl. *Mater. Res. Bull.*, *7*, 1281–1292.

Meier, W. M. and H. Villiger (1969) Die Methode der Abstandsverfeinerung zur Bestimmung der Atomkoordinaten idealisierter Gerüststrukturen. *Z. Kristallogr.*, *129*, 411–423.

Moore, P. B. (1966) The crystal structure of metastrengite and its relationship to strengite and phosphophyllite. *Am. Mineral.*, *51*, 168–176.

Rumanova, I. M. and M. N. Znamenskaya (1960) The crystal structure of anapaite. *Kristallografiya*, *5*, 681–688 [transl. *Sov. Phys. Crystallogr.*, *5*, 650–658 (1961)].

Shannon, R. D. and C. T. Prewitt (1969) Effective ionic radii in oxides and fluorides. *Acta Crystallogr.*, *B25*, 925–946.

Steinmetz, H. (1926) Phosphophyllit und Reddingit von Hagendorf. *Z. Kristallogr.*, *64*, 405–412.

Stewart, R. F., E. R. Davidson and W. T. Simpson (1965) Coherent X-ray scattering for the hydrogen atom in the hydrogen molecule. *J. Chem. Phys.*, *42*, 3175–3187.

Strunz, H. (1942) Isotypie unter Besetzung vakanter Gitterorte. $Fe_2^{\cdots}[PO_4]_2 \cdot 4H_2O$ und $Fe_3^{\cdot\cdot}[PO_4]_2 \cdot 4H_2O$. *Naturwissenschaften* *30*, 531–534.

Whitaker, A. (1975) The crystal structure of hopeite, $Zn_3(PO_4)_2 \cdot 4H_2O$. *Acta Crystallogr.*, *B31*, 2026–2035.

Wolfe, C. W. (1940) Classification of minerals of the type $A_3(XO_4)_2 \cdot nH_2O$. *Am. Mineral.*, *25*, 738–753, 787–809.

Manuscript received, December 13, 1976; accepted for publication, March 7, 1977.